EUROPEAN ORGANIZATION FOR NUCLEAR RESEARCH

CERN-PPE/91-61
April 4, 1991

A Search for Scalar Leptoquarks in Z^0 Decays

The OPAL Collaboration

Abstract

A search for scalar leptoquarks has been performed with data from the OPAL detector at the e^+e^- storage ring LEP. In a data sample corresponding to an integrated luminosity of $6.3 pb^{-1}$ no evidence for leptoquark production was observed where the leptoquark decays into a quark and either a charged lepton (e, μ, τ) or a neutrino. An upper limit of $1.7\,pb$ on the production cross section for leptoquarks is obtained assuming a branching ratio of 50% for the decay of the leptoquark into the channels with a charged lepton. Lower limits on the leptoquark mass between 41.4 and $46.4\,GeV/c^2$ at 95% CL are obtained, depending on the effective $SU(2) \times U(1)$ invariant couplings assigned to the leptoquark.

(Submitted to Physics Letters B)

The OPAL Collaboration

G. Alexander[23], J. Allison[16], P.P. Allport[5], K.J. Anderson[9], S. Arcelli[2], J.C. Armitage[6], P. Ashton[16], A. Astbury[a], D. Axen[b], G. Azuelos[18,c], G.A. Bahan[16], J.T.M. Baines[16], A.H. Ball[17], J. Banks[16], G.J. Barker[13], R.J. Barlow[16], J.R. Batley[5], G. Beaudoin[18], A. Beck[23], J. Becker[10], T. Behnke[8], K.W. Bell[20], G. Bella[23], S. Bethke[11], O. Biebel[3], U. Binder[10], I.J. Bloodworth[1], P. Bock[11], H.M. Bosch[11], S. Bougerolle[b], B.B. Brabson[12], H. Breuker[8], R.M. Brown[20], R. Brun[8], A. Buijs[8], H.J. Burckhart[8], P. Capiluppi[2], R.K. Carnegie[6], A.A. Carter[13], J.R. Carter[5], C.Y. Chang[17], D.G. Charlton[8], J.T.M. Chrin[16], P.E.L. Clarke[25], I. Cohen[23], W.J. Collins[5], J.E. Conboy[15], M. Cooper[22], M. Couch[1], M. Coupland[14], M. Cuffiani[2], S. Dado[22], G.M. Dallavalle[2], S. De Jong[8], P. Debu[21], M.M. Deninno[2], A. Dieckmann[11], M. Dittmar[4], M.S. Dixit[7], E. Duchovni[26], G. Duckeck[11], I.P. Duerdoth[16], D.J.P. Dumas[6], G. Eckerlin[11], P.A. Elcombe[5], P.G. Estabrooks[6], E. Etzion[23], F. Fabbri[2], M. Fincke-Keeler[a], H.M. Fischer[3], D.G. Fong[17], C. Fukunaga[24], A. Gaidot[21], O. Ganel[26], J.W. Gary[11], J. Gascon[18], R.F. McGowan[16], N.I. Geddes[20], C. Geich-Gimbel[3], S.W. Gensler[9], F.X. Gentit[21], G. Giacomelli[2], V. Gibson[5], W.R. Gibson[13], J.D. Gillies[20], J. Goldberg[22], M.J. Goodrick[5], W. Gorn[4], C. Grandi[2], E. Gross[26], J. Hagemann[8], G.G. Hanson[12], M. Hansroul[8], C.K. Hargrove[7], P.F. Harrison[13], J. Hart[5], P.M. Hattersley[1], M. Hauschild[8], C.M. Hawkes[8], E. Heflin[4], R.J. Hemingway[6], R.D. Heuer[8], J.C. Hill[5], S.J. Hillier[1], D.A. Hinshaw[18], C. Ho[4], J.D. Hobbs[9], P.R. Hobson[25], D. Hochman[26], B. Holl[8], R.J. Homer[1], S.R. Hou[17], C.P. Howarth[15], R.E. Hughes-Jones[16], R. Humbert[10], P. Igo-Kemenes[11], H. Ihssen[11], D.C. Imrie[25], L. Janissen[6], A. Jawahery[17], P.W. Jeffreys[20], H. Jeremie[18], M. Jimack[2], M. Jobes[1], R.W.L. Jones[13], P. Jovanovic[1], D. Karlen[6], K. Kawagoe[24], T. Kawamoto[24], R.K. Keeler[a], R.G. Kellogg[17], B.W. Kennedy[15], C. Kleinwort[8], D.E. Klem[19], T. Kobayashi[24], T.P. Kokott[3], S. Komamiya[24], L. Köpke[8], R. Kowalewski[6], H. Kreutzmann[3], J. von Krogh[11], J. Kroll[9], M. Kuwano[24], P. Kyberd[13], G.D. Lafferty[16], F. Lamarche[18], W.J. Larson[4], J.G. Layter[4], P. Le Du[21], P. Leblanc[18], A.M. Lee[17], M.H. Lehto[15], D. Lellouch[8], P. Lennert[11], C. Leroy[18], L. Lessard[18], S. Levegrün[3], L. Levinson[26], S.L. Lloyd[13], F.K. Loebinger[16], J.M. Lorah[17], B. Lorazo[18], M.J. Losty[7], X.C. Lou[12], J. Ludwig[10], M. Mannelli[8], S. Marcellini[2], G. Maringer[3], A.J. Martin[13], J.P. Martin[18], T. Mashimo[24], P. Mättig[3], U. Maur[3], T.J. McMahon[1], J.R. McNutt[25], F. Meijers[8], D. Menszner[11], F.S. Merritt[9], H. Mes[7], A. Michelini[8], R.P. Middleton[20], G. Mikenberg[26], J. Mildenberger[6], D.J. Miller[15], C. Milstene[23], R. Mir[12], W. Mohr[10], C. Moisan[18], A. Montanari[2], T. Mori[24], M.W. Moss[16], T. Mouthuy[12], P.G. Murphy[16], B. Nellen[3], H.H. Nguyen[9], M. Nozaki[24], S.W. O'Neale[8,d], B.P. O'Neill[4], F.G. Oakham[7], F. Odorici[2], M. Ogg[6], H.O. Ogren[12], H. Oh[4], C.J. Oram[e], M.J. Oreglia[9], S. Orito[24], J.P. Pansart[21], B. Panzer-Steindel[8], P. Paschievici[26], G.N. Patrick[20], S.J. Pawley[16], P. Pfister[10], J.E. Pilcher[9], J.L. Pinfold[26], D.E. Plane[8], P. Poffenberger[a], B. Poli[2], A. Pouladdej[6], E. Prebys[8], T.W. Pritchard[13], H. Przysiezniak[18], G. Quast[8], M.W. Redmond[9], D.L. Rees[1], K. Riles[4], S.A. Robins[13], D. Robinson[8], A. Rollnik[3], J.M. Roney[9], S. Rossberg[10], A.M. Rossi[2,f], P. Routenburg[6], K. Runge[10], O. Runolfsson[8], D.R. Rust[12], S. Sanghera[6], M. Sasaki[24], A.D. Schaile[10], O. Schaile[10], W. Schappert[6], P. Scharff-Hansen[8], P. Schenk[a], H. von der Schmitt[11], S. Schreiber[3], J. Schwarz[10], W.G. Scott[20], M. Settles[12], B.C. Shen[4], P. Sherwood[15], R. Shypit[b], A. Simon[3], P. Singh[13], G.P. Siroli[2], A. Skuja[17], A.M. Smith[8], T.J. Smith[8], G.A. Snow[17], R. Sobie[g], R.W. Springer[17], M. Sproston[20], K. Stephens[16], H.E. Stier[10], D. Strom[9], H. Takeda[24], T. Takeshita[24], P. Taras[18], S. Tarem[26], P. Teixeira-Diaz[11], N.J. Thackray[1], T. Tsukamoto[24], M.F. Turner[5], G. Tysarczyk-Niemeyer[11], D. Van den plas[18], R. Van Kooten[8], G.J. VanDalen[4], G. Vasseur[21], C.J. Virtue[19], A. Wagner[11], C. Wahl[10], J.P. Walker[1], C.P. Ward[5], D.R. Ward[5], P.M. Watkins[1], A.T. Watson[1], N.K. Watson[8], M. Weber[11], S. Weisz[8], P.S. Wells[8], N. Wermes[11], M. Weymann[8], M.A. Whalley[1], G.W. Wilson[21], J.A. Wilson[1], I. Wingerter[8], V-H. Winterer[10], N.C. Wood[16], S. Wotton[8], T.R. Wyatt[16], R. Yaari[26], Y. Yang[4,h], G. Yekutieli[26], I. Zacharov[8], W. Zeuner[8], G.T. Zorn[17].

[1]School of Physics and Space Research, University of Birmingham, Birmingham, B15 2TT, UK
[2]Dipartimento di Fisica dell' Università di Bologna and INFN, Bologna, 40126, Italy
[3]Physikalisches Institut, Universität Bonn, D-5300 Bonn 1, FRG
[4]Department of Physics, University of California, Riverside, CA 92521 USA
[5]Cavendish Laboratory, Cambridge, CB3 0HE, UK
[6]Carleton University, Dept of Physics, Colonel By Drive, Ottawa, Ontario K1S 5B6, Canada
[7]Centre for Research in Particle Physics, Carleton University, Ottawa, Ontario K1S 5B6, Canada
[8]CERN, European Organisation for Particle Physics, 1211 Geneva 23, Switzerland
[9]Enrico Fermi Institute and Department of Physics, University of Chicago, Chicago Illinois 60637, USA
[10]Fakultät für Physik, Albert Ludwigs Universität, D-7800 Freiburg, FRG
[11]Physikalisches Institut, Universität Heidelberg, Heidelberg, FRG
[12]Indiana University, Dept of Physics, Swain Hall West 117, Bloomington, Indiana 47405, USA
[13]Queen Mary and Westfield College, University of London, London, E1 4NS, UK
[14]Birkbeck College, London, WC1E 7HV, UK
[15]University College London, London, WC1E 6BT, UK
[16]Department of Physics, Schuster Laboratory, The University, Manchester, M13 9PL, UK
[17]Department of Physics and Astronomy, University of Maryland, College Park, Maryland 20742, USA
[18]Laboratoire de Physique Nucléaire, Université de Montréal, Montréal, Quebec, H3C 3J7, Canada
[19]National Research Council of Canada, Herzberg Institute of Astrophysics, Ottawa, Ontario K1A 0R6, Canada
[20]Rutherford Appleton Laboratory, Chilton, Didcot, Oxfordshire, OX11 0QX, UK
[21]DPhPE, CEN Saclay, F-91191 Gif-sur-Yvette, France
[22]Department of Physics, Technion-Israel Institute of Technology, Haifa 32000, Israel
[23]Department of Physics and Astronomy, Tel Aviv University, Tel Aviv 69978, Israel
[24]International Centre for Elementary Particle Physics and Dept of Physics, University of Tokyo, Tokyo 113, and Kobe University, Kobe 657, Japan
[25]Brunel University, Uxbridge, Middlesex, UB8 3PH UK
[26]Nuclear Physics Department, Weizmann Institute of Science, Rehovot, 76100, Israel
[§]University of British Columbia, Dept of Physics, 6224 Agriculture Road, Vancouver BC V6T 2A6, Canada
[§§]University of Victoria, Dept of Physics, P O Box 1700, Victoria BC V8W 2Y2, Canada

[a]Univ of Victoria, Victoria, Canada
[b]Univ of British Columbia, Vancouver, Canada
[c]and TRIUMF, Vancouver, Canada
[d]On leave from Birmingham University
[e]Univ of Victoria, and TRIUMF, Canada
[f]Present address: Dipartimento di Fisica, Università della Calabria and INFN, 87036 Rende, Italy
[g]Univ of British Columbia and IPP, Canada
[h]On leave from Research Institute for Computer Peripherals, Hangzhou, China

1 Introduction

The Standard Model does not contain any motivation for the generation structure of fermions or for the symmetry between quarks and leptons. In order to explain such properties, models based on Grand Unified Theories, Superstrings, or Compositeness have been proposed which require new kinds of interactions and new types of particles. Several of these models [1] predict the existence of leptoquarks χ, a new type of particles carrying lepton number as well as baryon number. This paper reports on the search for leptoquarks in Z^0 decays recorded with the OPAL detector at the e^+e^- collider LEP. The search is restricted to scalar leptoquarks which are assumed to be their lightest representatives.

The prediction of both the production and decay mechanisms of leptoquarks depends on the specific model used. However, for leptoquarks with mass below $45\,GeV/c^2$ which can be pair-produced at LEP, some of the couplings are constrained by low energy measurements [2]. For example the absence of $K^+ \to \pi^+\nu\nu$ or $D^0 \to \mu^+\mu^-$ decays constrains the non-diagonal terms in the coupling matrix of χ to quarks and leptons to about 5×10^{-5} for the first two generations. The magnitudes of the third generation couplings are not constrained by these measurements since these terms are not accessible at low energies. In addition, some models propose a mass dependent coupling $\lambda_{\chi ql} \sim 1/2\sqrt{m_q \cdot m_l}/M_W$ allowing larger off diagonal terms for the third generation. In this letter the restriction for leptoquarks to decay only within one generation of fermions is called family diagonal. As this restriction decouples the fermion families, it implies the existence of a family structure also for leptoquarks.

The production yield in e^+e^- collisions is given by the coupling of χ to the photon and to the Z^0. Whereas the coupling to the photon is unambiguously given by the electric charge, the coupling to the Z^0 depends on the weak group structure of leptoquarks. The quantum numbers of leptoquarks with effective $SU(2) \times U(1)$ invariant couplings are summarized in [3]. The smallest coupling occurs for a weak isosinglet charge $1/3$ leptoquark which yields about 3×10^{-5} of the hadronic cross section on the Z^0 resonance. Leptoquarks with electron quantum number can also be produced or exchanged in the t-channel. Such processes were not considered in the current analysis as their cross sections are negligible.

Based on the above assumptions, only family diagonal decays were considered in the first two generations and family mixing decays were allowed in the third generation. Therefore rare decays of the Z^0 of the type $Z^0 \to l\bar{l}q\bar{q}$ were searched for, where the l's are either neutrinos or charged leptons: e, μ or τ's. Assuming lepton number conservation in the $\chi\bar{\chi}$ production both leptons are from the same generation. The family mixing in the third generation allows decays of the type $\chi\bar{\chi} \to \tau^+\nu_\tau q_{2/3}\bar{q}_{1/3}$, which would otherwise require the decay into a t-quark, inaccessible at LEP. Since the leptoquarks decay into either νq or lq events of the following topologies were sought:

- Jets with two isolated charged leptons.
- Jets with one isolated charged lepton and missing energy.
- Jets with missing energy.

No effort was made to identify the quark species.

Previous searches at other e^+e^- colliders set a lower limit of $28\,GeV/c^2$ on the mass of a scalar leptoquark [4]. Experiments at $p\bar{p}$ colliders [5] exclude leptoquarks decaying into muons with masses up to about $35\,GeV/c^2$. The present search is sensitive to masses up to about $45\,GeV/c^2$.

After a short description of the OPAL detector the event selection for this analysis is summarized. Then the search for leptoquarks in the various event topologies is presented. The non observation of a signal is translated into limits on the leptoquark mass and on the production cross section.

2 The OPAL Detector

This analysis is based on the central tracking chambers, the electromagnetic calorimeter and the muon detection system of the OPAL detector [6]. The central tracking system provides up to 183 space points per track and close to 100% tracking efficiency for charged tracks in the polar angle range defined by $|\cos\theta| < 0.92$. High energy tracks are measured with a momentum resolution $\sigma(p)/p^2 \approx 2.2 \times 10^{-3}$ GeV^{-1}. The electromagnetic calorimeter consists of a cylindrical array of 9,440 lead glass blocks in the barrel region ($|\cos\theta| < 0.82$) and 2,264 lead glass blocks in the two endcap regions ($0.81 < |\cos\theta| < 0.98$). It has a typical energy resolution of $\Delta E/E \approx 3\%$ for $E \approx 45\,GeV$. The hadron calorimeter consists of 9 layers (8 layers in the endcap region) of limited streamer tubes interleaved with 10 cm iron slabs. Muons are identified by the hadron calorimeter and by four layers of muon chambers surrounding the hadron calorimeter. The OPAL detector covers about 98% of the solid angle and measures the visible energy with a resolution of typically 11% thus providing a good measurement of missing momentum.

3 The Data Sample

The data used in this analysis correspond to an integrated luminosity of $6.3\,pb^{-1}$ equivalent to about 160,000 visible Z^0 decays, recorded at centre of mass energies between 88.2 and 94.3 GeV.

The decay of two leptoquarks leads preferentially to final states with a high multiplicity and a large energy deposition. To preselect such events the following criteria were applied:

- An event had to contain more than 5 charged tracks. Each track had to have more than 50% of the possible number of measured space points and at least 20 measured space points. The transverse momentum of the tracks with respect to the beam axis had to be more than 0.1 GeV/c. Their distance of closest approach to the interaction point had to be less then 2.5 cm in the plane transverse to the beam axis ($|\,d_0\,|$) and less than 50 cm along the beam direction ($|\,z_0\,|$).
- The scalar sum of all charged track momenta had to exceed 10 GeV/c.
- An event had to contain more than 8 separate energy depositions (clusters) in the leadglass calorimeter. The energy of each cluster had to exceed 170 MeV in the barrel region and 250 MeV in the endcap region.
- The total electromagnetic energy had to exceed 10 GeV.
- The thrust axis was required to be well contained in the detector by demanding that the polar angle Θ_{thrust} satisfied $|\cos\Theta_{thrust}| < 0.9$. To calculate the event thrust, both tracks and electromagnetic clusters were used.

In the initial data set of approximately 160,000 visible Z^0 decays these criteria were fulfilled by 124,459 events. This event sample was used for the search of leptoquark topologies with two isolated leptons.

For the decay channels with at least one neutrino, additional cuts were applied to select events with an observed energy imbalance. This selection which, at the same time rejected background processes yielding unobserved energy due to neutrinos and particles escaping along the beampipe, followed closely the one applied in a previous publication on the search for Higgs particles [7]:

- An energy imbalance in the plane transverse to the beam of $p_\perp^{vis} > 6\,GeV/c$ was required. The method of calculating the visible energy is described in [7]. It minimizes potential double counting of particle energies in the electromagnetic calorimeter and the tracking chambers.
- To eliminate the potential tau pair background, events with less than 9 charged tracks were required to have thrust below 0.95.
- The total energy deposit in the forward calorimeter covering the polar angle from 47 to 120 *mrads* had to be less than $2\,GeV$.
- In the region defined by $|\cos\theta| > 0.90$ the energy deposit in the lead glass calorimeter had to be less than 35% of the total electromagnetic energy seen in the calorimeter.
- The missing energy ($E_{miss} = E_{cm} - E_{vis}$) was required to be larger than zero and the polar angle of the missing momentum vector was required not to point into the forward direction ($|\cos\theta| < 0.90$).

This tighter preselection reduced the number of events to 37,158.

The decay of a heavy leptoquark into a quark and a charged lepton gives rise to the distinctive signature of an isolated lepton with an energy of typically half the beam energy. Correspondingly the decay into a quark and a neutrino leads to a missing energy of about half the beam energy. In both cases the leptons are typically isolated from the rest of the event.

In searching for the decay mode with charged leptons, all tracks were considered that have a momentum between $4\,GeV/c$ and $70\,GeV/c$, which originate from the interaction point ($|z_0| < 20\,cm$) and which have an associated cluster in the electromagnetic calorimeter. These tracks were then required to be isolated from all jets formed in the residual event by the cluster algorithm of [8]. A cut-off parameter $d_{join} = 2.5\,GeV$ was used. The signal efficiency is almost independent of the choice of d_{join}. As a measure of isolation, the quantity

$$\rho = \min_{j \in \{jets\}} [E_l\,(1 - \cos\Theta_{l,j})]^{1/2}\,. \tag{1}$$

was used. Here E_l is the energy of the track considered and $\Theta_{l,j}$ its angle to jet j. Higher isolation is defined by a larger value of ρ. An equivalent procedure was used for the isolation of the missing momentum, replacing the track momentum by the missing momentum vector.

The distribution of ρ for all charged tracks and for the missing momentum is shown in figure 1 together with the predictions of the JETSET parton shower Monte Carlo for standard multihadronic events [9]. The generated events were processed through a detailed simulation of the OPAL detector [10] and reconstructed in the same way as the data. The ρ-distributions are steeply decreasing with increasing ρ. For charged tracks the distribution flattens out for ρ above $3\,GeV^{1/2}$ due to contributions from jets consisting of a single track. The measured distributions show reasonable agreement with the expectations for multihadronic events.

Experimental checks were performed to evaluate the systematic uncertainties affecting the efficiency of finding isolated tracks and the quality of the reconstruction of the missing momentum. The effect

of the track quality cuts on the efficiency to find isolated tracks has been measured with 2 prong $\tau^+\tau^-$ events collected during the same running period. The average efficiency was found to be 96.7%, varying by 1.8% over the momentum range of the leptoquarks. This variation was taken as the systematic error due to tracking efficiency. The degradation of the efficiency by potential overlaps from additional tracks in the central detector is negligible. To study the experimental resolution in missing momentum, multihadronic events with an isolated photon [11] were used. Excluding the photon from the calculation of the missing momentum, the isolation of the missing momentum was compared with the isolation parameter of the photon giving a resolution of $\sigma(\rho_{miss})/\rho_{miss} \approx 30\%$. This resolution is well represented by the simulation.

4 Search for Leptoquark Decays

Each of the decay topologies of a pair of leptoquarks had been searched for separately. This allows the efficiency to be calculated for any combination of branching ratios $f_c = BR(\chi \to lq)$ and $f_n = BR(\chi \to \nu q)$ for the leptoquarks to decay into charged and neutral leptons respectively. With ϵ_{cc}, ϵ_{cn} and ϵ_{nn} being the efficiency of detecting the decays with two charged leptons, a charged lepton and a neutrino and two neutrinos respectively, the total efficiency reads

$$\epsilon(m_\chi, f_c, f_n) = f_c^2\epsilon_{cc}(m_\chi) + 2f_cf_n\epsilon_{cn}(m_\chi) + f_n^2\epsilon_{nn}(m_\chi) \tag{2}$$

(note $f_c + f_n = 1$).

The efficiencies were determined by simulating leptoquark production for which the differential cross section is given [13] by

$$\frac{d\sigma}{d\cos\theta} = \frac{3}{4}\beta^3 \sin^2\theta \left(\frac{\pi\alpha^2}{s} e_\chi^2 - \frac{\alpha G_\mu}{\sqrt{2}} e_\chi c_\chi v_e \frac{m_Z^2(s-m_Z^2)}{D(s)} + \frac{G_\mu^2}{8\pi} c_\chi^2(v_e^2+a_e^2)\frac{s\,m_Z^4}{D(s)} \right) \tag{3}$$

Here $\beta = p/E$ is the velocity of the leptoquark, s the square of the centre of mass energy, $D(s) = (s-m_Z^2)^2 + (\Gamma_Z m_Z)^2$, $v_e = -1 + 4\sin^2\theta_W$ and $a_e = -1$ are the vector and axial couplings of the electron, e_χ and c_χ are the charge and coupling of the leptoquark to the Z^0, and α and G_μ are the electromagnetic and Fermi couplings. The differential cross section was folded with the effect of initial state radiation [12], which reduced the cross section by about 30%. The leptoquarks were then made to decay isotropically into leptons and quarks. The two quark system in the final state was hadronized according to JETSET7.2. Finally the response of the detector was simulated.

Based on this simulation the shape of the expected ρ distribution for a leptoquark of $40\,GeV/c^2$ mass is displayed in figure 1. Both for the charged and the neutral decay mode the leptoquark signal is seen to extend to very large values of ρ due to the presence of isolated tracks and neutrinos.

The following discussion is divided into the search for leptoquarks which decay into electrons or muons and those that decay into taus. This separation is motivated by the much less pronounced signature due to the tau decay with its predominant hadronic decay modes and its reduced visible energy.

4.1 Search for $\chi\bar{\chi} \to (e^+e^-$ or $\mu^+\mu^-)q\bar{q}$

Two isolated oppositely charged tracks were required. The most isolated track had to satisfy $\rho_1 > 1.8\,GeV^{1/2}$ and had to be identified as an electron or a muon as follows:

- Electrons were identified by their response in the electromagnetic calorimeter. An electron candidate with momentum p had an associated energy deposit E in the electromagnetic calorimeter satisfying $0.75 < E/p < 2$.
- A central detector track with an associated track "segment" in the muon detector was classified as a muon. Muon segments were associated to a charged track if the difference of the extrapolated azimuthal angle ϕ of the track and the muon segment was less then $100\,mrad$.

From the 124,459 preselected events 69 were retained, to be compared to 62 ± 8 events expected from the simulation of multihadronic events.

The ρ_2-distribution of tracks with the second largest isolation is shown in figure 2a) for the 69 events, for the expectation for multihadrons, and for a leptoquark of $40\,GeV/c^2$ mass. Whereas neither in the data, nor in the simulated multihadronic sample, are there any tracks with $\rho_2 > 0.7\,GeV^{1/2}$, leptoquarks have large values of ρ_2 extending up to $\rho_2 \sim 6\ GeV^{1/2}$. Requiring the second isolated track to have $\rho_2 > 1.0\,GeV^{1/2}$ removed all events in the data, while retaining about 60% ($= \epsilon_{cc}$) of the $Z^0 \to \chi\bar{\chi}$ decays. Table 1 shows the number of data events after the cuts, the expectations from the simulated multihadronic events and the signal efficiencies for the above requirements. In table 4 the efficiencies are listed as a function of the leptoquark mass.

In figure 1a), the slight excess of data for ρ-values in the range $1-2\,GeV^{1/2}$ indicates that the simulation tends to underestimate the isolation of tracks. Assuming that this also holds for leptoquarks, the signal efficiencies obtained from the simulation are rather conservative. The signal efficiency is affected by a systematic error due to the lepton identification. The efficiencies were obtained from e^+e^- and $\mu^+\mu^-$ - pairs and found to be 89.5±1.0% and 86.2±1.3% respectively. The variation of the efficiency with momentum was obtained from a simulation; it was found to be 3%. Combined with the uncertainty in the tracking efficiency this resulted in a total systematic error of 4% for this selection.

4.2 Search for $\chi\bar{\chi} \to (e\nu$ or $\mu\nu)q\bar{q}$

In addition to a single isolated lepton these events would contain a substantial amount of missing energy escaping with the neutrino. Therefore the tighter event preselection described above was used. By demanding an isolated electron or muon candidate with $\rho > 1.8\,GeV^{1/2}$ 31 events were retained, to be compared to 27 ± 5 multihadronic events expected from the simulation.

Just as for the charged lepton, the missing momentum vector is, in general, isolated from the rest of the event. To select a possible leptoquark signal, *either* the isolation of the missing momentum had to be $\rho_{miss} > 1.5\,GeV^{1/2}$ *or* the requirement on the isolated charged particle was tightened to $\rho > 4\,GeV^{1/2}$. This left 5 events to be compared to the expectation of 6 ± 2 events. The neutrino also tends to give rise to an acolinear event structure. The acolinearity was measured by the angle α between the total momentum vector of all particles in the two hemispheres which were defined with respect to the thrust axis. The requirement $\theta_{acol} = 180 - \alpha < 10°$ removed the remaining events in the data while the simulation of multihadronic events predicted one event. The signal efficiency for a potential leptoquark decay $Z^0 \to \chi\bar{\chi} \to q\bar{q}l^{\pm}\nu$ was close to 50%. The effect of the cuts on the data, on the simulation of multihadronic events, and on the signal, can be found in table 2, the dependence on the leptoquark mass in table 4. The efficiency decreases with leptoquark mass due to the acolinearity requirements; it shows a maximum for leptoquark masses of about $40\,GeV/c^2$.

The systematic error on the efficiency of this selection is dominated by the error on lepton identification and by the quality of the reconstruction of the missing momentum vector. Increasing the

cut on ρ_{miss} by 30% which corresponds to the missing momentum resolution, decreased the signal efficiency by 4%. This variation was considered as the systematic error due to ρ_{miss}. Combining it with the other errors gave a total uncertainty of 5.4%.

4.3 Search for $\chi\bar{\chi} \to (\tau^+\tau^-$ or $\tau\nu)q\bar{q}$

The predominant decay modes of the tau into one charged particle and neutrals leads to a less energetic charged track than seen in the electron and muon decay modes of the leptoquark. Since two or more neutrinos are expected, the events are characterized by a substantial amount of missing energy and momentum imbalance. Again the tighter event preselection defined above was used. To select the possible leptoquark signal, one isolated track with $\rho_{CD} > 1.5\,GeV^{1/2}$ was required. The index indicates, that the isolation was this time calculated using charged tracks only, to allow tau candidates to have close by neutral energy, predominantly due to π^0. In addition to the momentum and track quality requirements, candidate tracks with an additional good track closer than 15° were discarded. These cuts retained 1140 events while the simulation of multihadronic events predicted 967 ± 28 events (see table 3).

Within multihadronic events, tracks surviving these cuts can be due to one quark or gluon fragmenting very hard or to a substantial amount of neutral hadronic energy accompanying a single track. Such low-multiplicity 'jets' are mostly colinear with the event axis and could be eliminated by requiring $|\cos\theta_{TA}| < 0.98$. Here θ_{TA} is the angle of the track to the thrust axis.

To improve the isolation measurement for the taus, the following procedure was used. The charged and electromagnetic energy in a cone of 15° half angle around the track was summed up and the invariant mass from this energy and momentum sums was calculated. To retain only potential tau candidates the invariant mass was required to be less then $1.5\,GeV$. For the tau candidates which consisted of the merged track and electromagnetic clusters the isolation parameter (ρ^τ) was calculated as usual, considering both charged tracks *and* electromagnetic clusters.

Leptoquarks decaying into two taus were selected by demanding two oppositely charged tracks satisfying the above requirements. This left 25 events in the data, whereas JETSET predicted 15 ± 4 events. In addition it was required, either that the τ candidate with the second highest isolation satisfies $\rho_2^\tau > 1.5\,GeV^{1/2}$ or that the acolinearity angle of the event be larger than 18°. The correlation of θ_{acol} and ρ_2^τ is displayed in figure 2c). Whereas the data is clustered at low ρ_2^τ and low θ_{acol}, leptoquarks are expected to contribute at large acolinearities and large values of ρ. No event was found satisfying the requirements while 11.3% of the $\chi\bar{\chi} \to \tau^+\tau^- q\bar{q}$ decays passed the selection. From the simulation of multihadronic events a background of 2.5 ± 1.4 events was expected. The systematic uncertainties are mainly due to the track quality requirements. From a comparison of the invariant mass distribution for tau pair events in data and simulation, the error on the invariant mass cut was found to be negligible. The dependence of the efficiency on the leptoquark mass can be found in table 4. The efficiency for a $25\,GeV/c^2$ leptoquark is seen to be 50% lower than that for a $40\,GeV/c^2$ leptoquark; this is due to the requirement on the angle of the tau candidate to the thrust axis.

Since leptoquarks of mass below $46\,GeV/c^2$ which are considered in this analysis can not decay into top quarks, the decay $Z^0 \to \chi\bar{\chi} \to l\nu q\bar{q}$ with all fermions in the third generation is forbidden. The decay topology $\tau\nu_\tau q\bar{q}$ can only occur if one relaxes the restriction to family diagonal couplings $\lambda_{\chi q\tau}$. There are no strong experimental constraints for such couplings in the third generation; furthermore, as outlined in the introduction, the decay $\chi \to \tau\nu_\tau b\bar{c}$ can be sizeable because of the higher masses of the decay products involved.

The decay into one tau and one neutrino was selected by demanding at least one charged track with the above properties. In addition $\rho_{miss} > 3.5 GeV^{1/2}$ and an acolinearity angle $\theta_{acol} > 26°$ was required. This selected 17% of the $\chi\bar{\chi} \to \tau\nu q\bar{q}$ events and discarded all events in the data.

4.4 Search for $\chi\bar{\chi} \to \nu\bar{\nu}q\bar{q}$

Because of the almost identical topology, the analysis of the leptoquark channel involving two neutrinos followed exactly the search of this collaboration for the Higgs boson, in the process $Z^0 \to H^0 Z^{0*}$; $Z^{0*} \to \nu\bar{\nu}$ [7]. The cuts used in this analysis are summarized below:

- An acoplanar event structure was demanded by selecting events with $\beta < 164°$, where β is the angle between the momentum vectors of the two hemispheres (defined by the thrust axis) projected on the plane perpendicular to the beam axis. In addition, the three dimensional acolinearity angle was required to be $\alpha < 154°$.
- The missing momentum vector was required to be isolated by demanding less than $2\,GeV$ of electromagnetic and charged energy in a cone of 30° half angle around the missing momentum vector.
- The average $(M_1 + M_2)/2$ of the two effective masses corresponding to the two hemispheres had to be less than $12.5\,GeV$ or the energy in one of the hemispheres had to be less than $3\,GeV$. The first cut selects events with only one jet in each hemisphere, the second cut those events where both jets are in one hemisphere.

After these cuts no events were retained. The efficiency of detecting two leptoquarks each of which decays into a neutrino, is typically 60% and is listed in table 4 for various leptoquark masses. As in [7], the systematic uncertainties in the selection procedure were dominated by the simulation of the detector response (2%) and fragmentation dependence (3%), giving a total uncertainty of 4% on the efficiency.

5 Limits on Leptoquark Production

From the absence of a signal for leptoquarks, limits can be set on their production cross section (σ_{lim}). For the broad range of possible couplings to the Z^0 these limits can be interpreted in terms of the mass range, the coupling c_χ to the Z^0 and the branching fractions. The maximum allowed cross section for leptoquarks is given by

$$\sigma_{lim} = \frac{1}{L}\left(\frac{N_{CL}}{\epsilon_{nn} f_n^2 + 2\epsilon_{nc} f_n f_c + \epsilon_{cc} f_c^2}\right) \tag{4}$$

where the ϵ_{ij} is the efficiency of detecting the topology ij and f_i is the branching ratio of a leptoquark decay ($i, j = n, c$). The indices n and c denote the neutral and the charged mode respectively. N_{CL} is the number of events corresponding to the chosen confidence limit, and L the integrated luminosity of the data sample. Since no potential leptoquark event had been found, N_{CL} was taken as three events yielding a 95% confidence upper limit. As a conservative approach, no background subtraction was performed in calculating the confidence limits.

In calculating the limiting cross section, the detection efficiencies have been reduced by the estimated systematic error. In addition to the errors for the various selection procedures, an error of 1.6% for the luminosity measurement was taken into account.

The σ_{lim} was then calculated for various branching ratios of the leptoquark decay and compared to the expectation assuming specific couplings of the leptoquark to the Z^0. Assuming $c_\chi = \frac{1}{3} sin^2\theta_W$, which gives the lowest coupling to the Z^0 [3], leptoquarks decaying into electrons or muons with masses up $44.2\,GeV/c^2$ are excluded, almost independently of the branching ratio. For leptoquarks decaying exclusively into taus, the mass limit is lower ($41.4\,GeV/c^2$, see figure 3a)).

Alternatively, fixing the branching ratio $BR(\chi \rightarrow l^{\pm}q)$=0.5 the upper limit of the cross section in terms of c_χ is given in figure 3b) as a function of m_χ. In table 5 the mass limits corresponding to the most general possible assignments of charge and weak isospin [3] to leptoquarks are listed. For leptoquarks decaying within one of the first two generations, the lowest efficiency obtained for a branching ratio $f_e = f_n = 50\%$ was used to calculate the mass limit. As these limits are almost identical for the two generations only one number is quoted.

For the leptoquark decaying into taus, the limits are given for the branching ratios $f_e = 50\%$ and 100%. For the case that only family diagonal decays occur for leptoquarks of the third generation, the charge of the leptoquark is restricted to values of $|q_\chi| = 2/3$ or $4/3$ and the branching ratio f_e to 100% or to zero. For these cases a lower limit of $45.0\,GeV/c^2$ is obtained.

In conclusion, no evidence has been found for leptoquark production in Z^0 decays. Searches have been performed for decays into all 3 generations of fermions, yielding lower limits at 95% confidence level of about $44.2\,GeV/c^2$ for the leptoquark mass. Thus the previous mass limits have been extended and also stringent limits on third generation leptoquarks have been provided. Similar limits were obtained in [14].

Acknowledgments

Our special thanks go to R.Rückl for his continuous theoretical advice and suggestions. In addition we are grateful to P.Zerwas for discussions and clarifying remarks.

It is a pleasure to thank the SL Division for the efficient operation of the LEP accelerator and their continuing close cooperation with our experimental group. In addition to the support staff at our own institutions we are pleased to acknowledge the following :
The Bundesministerium für Forschung und Technologie, FRG.
Department of Energy, USA
National Science Foundation, USA
Science and Engineering Research Council, UK
Natural Sciences and Engineering Research Council,Canada
Israeli Ministry of Science
Minerva Gesellschaft
The Japanese Ministry of Education, Science and Culture (the Monbusho) and a grant under the Monbusho International Science Research Program.
American Israeli Bi-national Science Foundation.
Direction des Sciences de la Matière du Commissariat à l'Energie Atomique, France.
and The A.P. Sloan Foundation.

References

[1] H. Georgi and S.L.Glashow, Phys. Rev. Lett **32** (1974) 438; J.C. Pati and A. Salam, Phys. Rev. **D10** (1974) 275; B. Schrempp, preprint MPI-PAE/Pth 72/86; L.F. Abbott and E. Farhi, Phys. Lett. **B101** 69; P. Langacker, Phys. Rep. **72** (1981) 185.

[2] W. Buchmüller and D. Wyler, Phys. Lett. **B177** (1986) 377.

[3] W. Buchmüller, R. Rückl and D. Wyler, Phys. Lett. **B191** (1987) 442.

[4] A. Miyamoto, Search for New Particles at TRISTAN, Recontres de Moriond, Electroweak session, Les Arcs, March 1990.

[5] S. Geer (UA1 Collab.), Constraints on Physics beyond the Standard Model, Europhysics conference on High Energy Physics, Uppsala, June 25. - July 1., 1987.

[6] OPAL Collab., K. Ahmet *et al.*, CERN-PPE/90-114 (1990) (submitted to Nucl. Instr. and Meth.)

[7] OPAL Collab., M.Z. Akrawy *et al.*, Phys. Lett. **B253** (1991) 511.

[8] T. Sjöstrand, JETSET version 7.2, CERN long write up.

[9] T. Sjöstrand, Comp. Phys. comm. **39** (1986) 347; T. Sjöstrand, Comp. Phys. comm. **43** (1987) 367; M. Bengtson and T. Sjöstrand, Nucl. Phys. . **B289** (1987) 810;

[10] J. Allison *et al*, Comp. Phys. Comm. **47** (1987) 55; R. Brun *et al*, GEANT3, CERN DD/EE/84-1 (1987).

[11] OPAL Collab., M.Z. Akrawy *et al.*, Phys. Lett. **B246** (1989) 285.

[12] G. Burgers, Shape and size of the Z resonance, in Polarization at LEP, CERN 88-06.

[13] J.L. Hewett and T.G. Rizzo, Phys. Rev. **D36** (1987) 3367.

[14] L3 Collab., B. Adeva *et al.*, L3 Preprint #26 (revised version) March 1991.

Tables

Cut	Events in data	JETSET prediction	Efficiency [%] for 40 GeV/c^2 Leptoquark electron	muon
Preselection	124459		89.1	
track pair, $\rho_1 > 1.8\,GeV^{1/2}$	441	322 ± 18	75.5	
ident. Lepton	69	62 ± 8	67.5	65.1
$\rho_2 > 1.0\,GeV^{1/2}$	0	0	59.6	57.4

Table 1: Effects of the cuts upon the search for two isolated leptons. Here and in the following tables the JETSET prediction is normalized to the 124459 preselected events.

Cut	Events in data	JETSET prediction	Efficiency [%] for 40 GeV/c^2 Leptoquark electron	muon
tight Preselection	37158	34468 ±186	69.8	
event with $\rho_1 > 1.8 GeV^{1/2}$	144	111 ± 11	61.1	
ident. Lepton	31	27 ± 5	54.6	52.7
$\rho_{miss} > 1.5\,GeV^{1/2}$				
or $\rho_1 > 4.0\,GeV^{1/2}$	5	6 ± 2	53.1	51.3
$\theta_{acol} > 10°$	0	1	49.9	48.1

Table 2: Effects of the cuts upon the search for one isolated lepton.

Cut	Events in data	JETSET prediction	Efficiency [%] for 40 GeV/c^2 Leptoquark
tight Preselection	37158	34468 ±186	60.6
event with $\rho_{CD} > 1.5 GeV^{1/2}$	1140	967 ± 28	39.0
τ candidates	465	384 ± 18	35.8
track pairs	25	15 ± 4	13.7
$\theta_{acol} > 18°$			
or $\rho_2^\tau > 1.5\,GeV^{1/2}$	0	2.5 ± 1.4	11.3

Table 3: Effects of the cuts upon the search for isolated taus.

$mass\ [GeV/c^2]$	25	30	35	40	45	typ. stat. error
$\chi \rightarrow$ electron + quark						
ϵ_{cc}	64.1	63.6	63.1	59.6	57.8	1.5
ϵ_{cn}	39.9	46.4	48.4	49.9	46.8	1.8
$\chi \rightarrow$ muon + quark						
ϵ_{cc}	61.8	61.2	60.9	57.4	55.6	1.5
ϵ_{cn}	38.8	44.8	47.6	48.1	45.2	1.8
$\chi \rightarrow \tau$ + quark						
ϵ_{cc}	5.1	8.3	8.6	11.3	10.2	0.7
ϵ_{cn}	21.2	26.3	22.1	17.2	12.1	1.2
$\chi \rightarrow \nu$ + quark						
ϵ_{nn}	47.4	50.7	58.3	62.4	66.1	1.6

Table 4: The lepton selection efficiencies ϵ_{cc} ϵ_{cn} and ϵ_{nn} (in %) as defined in the text, as a function of the leptoquark mass.

Weak			mass limit $[GeV/c^2]$		
isospin	T_3	Q_{em}	$\chi \rightarrow e, \mu$ all BR	$BR(\chi \rightarrow \tau) = 100\%$	$BR(\chi \rightarrow \tau) = 50\%$
0	0	-1/3	44.2	41.4	43.2
0	0	-4/3	45.5	45.0	43.3
1	+1	2/3	46.4	45.8	46.1
	0	-1/3	44.2	41.4	43.2
	-1	-4/3	46.3	45.5	46.0
1/2	+1/2	-2/3	46.2	45.5	45.9
	-1/2	-5/3	45.1	44.0	44.8
1/2	+1/2	1/3	45.9	45.3	45.5
	-1/2	-2/3	45.7	45.1	45.4

Table 5: Mass limits for all possible assignments of charge and weak isospin to leptoquarks with effective $SU(2) \times U(1)$ invariant couplings. The Z^0 coupling of the leptoquarks is given by $c_\chi = T_3 - Q_{em} \sin^2 \theta_W$ [3] .

Figures

Figure 1: a) The inclusive ρ distribution (multiple entries per event) for all tracks satisfying the quality requirements; b) ρ_{miss} distribution (one entry per event) for events with missing momentum passing the tight preselection for the data and the expectation from multihadronic events. The expectation from a leptoquark of mass $40\,GeV/c^2$ is shown with arbitrary normalisation

Figure 2: a) Isolation parameter ρ_2 of second isolated track (preselected with $\rho_1 > 1.8\,GeV$ and satisfying lepton identification criteria): for data, expectation from simulated multihadronic events and leptoquarks; b) Effect of the last cut on the acolinearity angle θ_{acol} for the data and the Monte Carlo prediction for multihadronic events and leptoquarks.
c) The acolinearity angle θ_{acol} vs. isolation parameter ρ_2^τ of second isolated track for data (open symbols) and leptoquarks.

Figure 3: a) Mass limit vs. branching ratio for $q_\chi = 1/3$, $T_3 = 0$; b) Excluded masses and couplings in units of lowest coupling $\frac{1}{3}\sin^2\theta_W$.

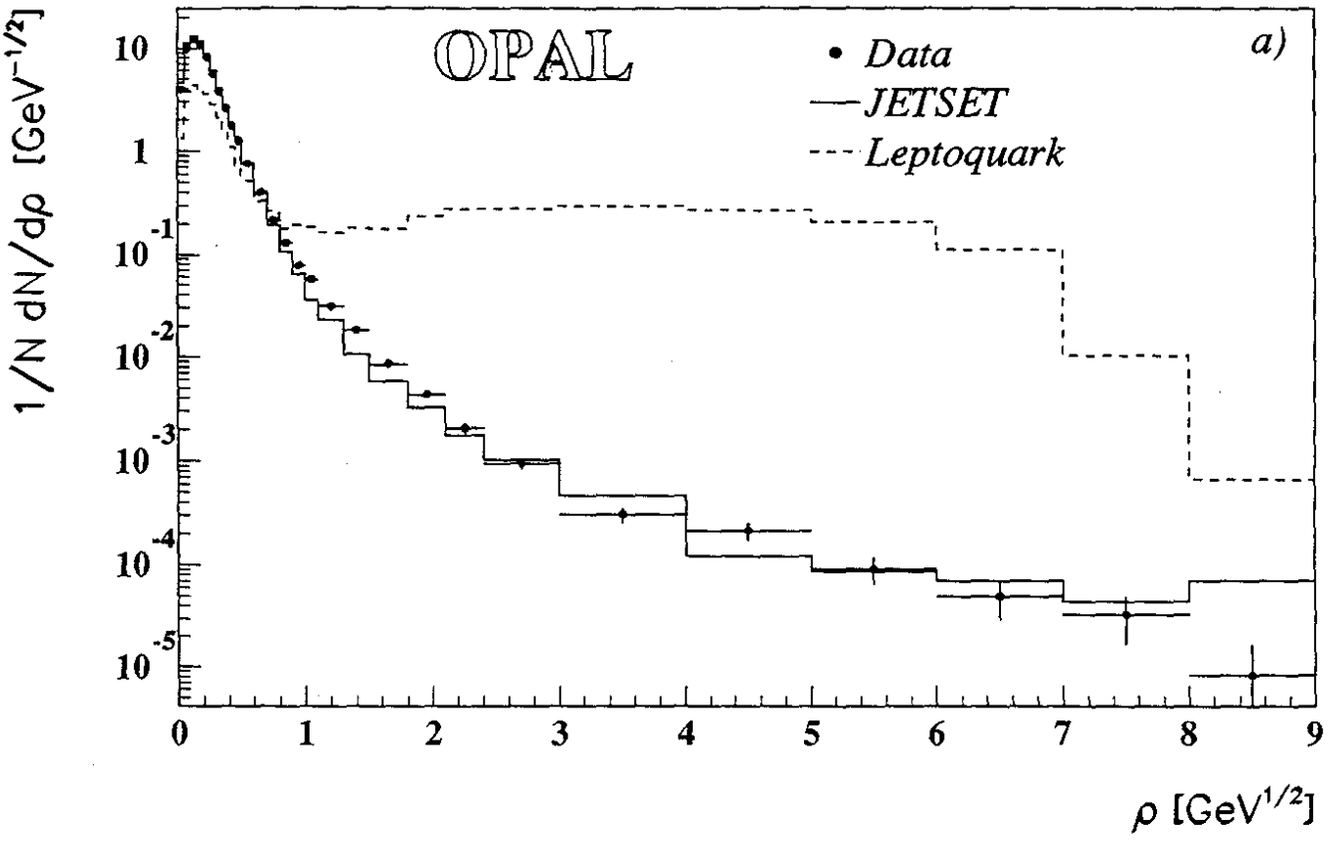
OPAL
• Data
—JETSET
---Leptoquark
a)
1/N dN/dρ [GeV^-1/2]
ρ [GeV^1/2]

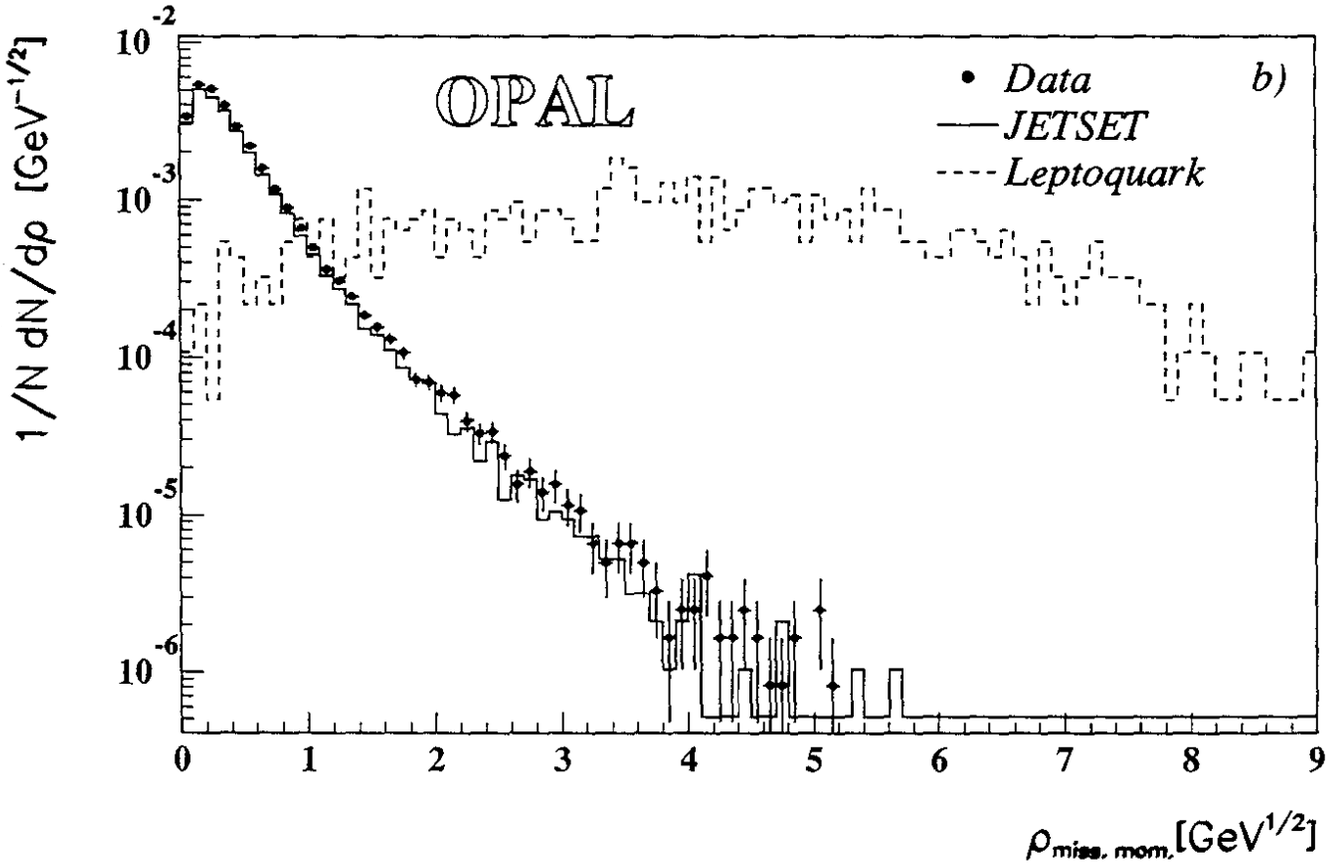
OPAL
• Data
—JETSET
----Leptoquark
b)
1/N dN/dρ [GeV^-1/2]
ρ miss. mom. [GeV^1/2]

Figure 1

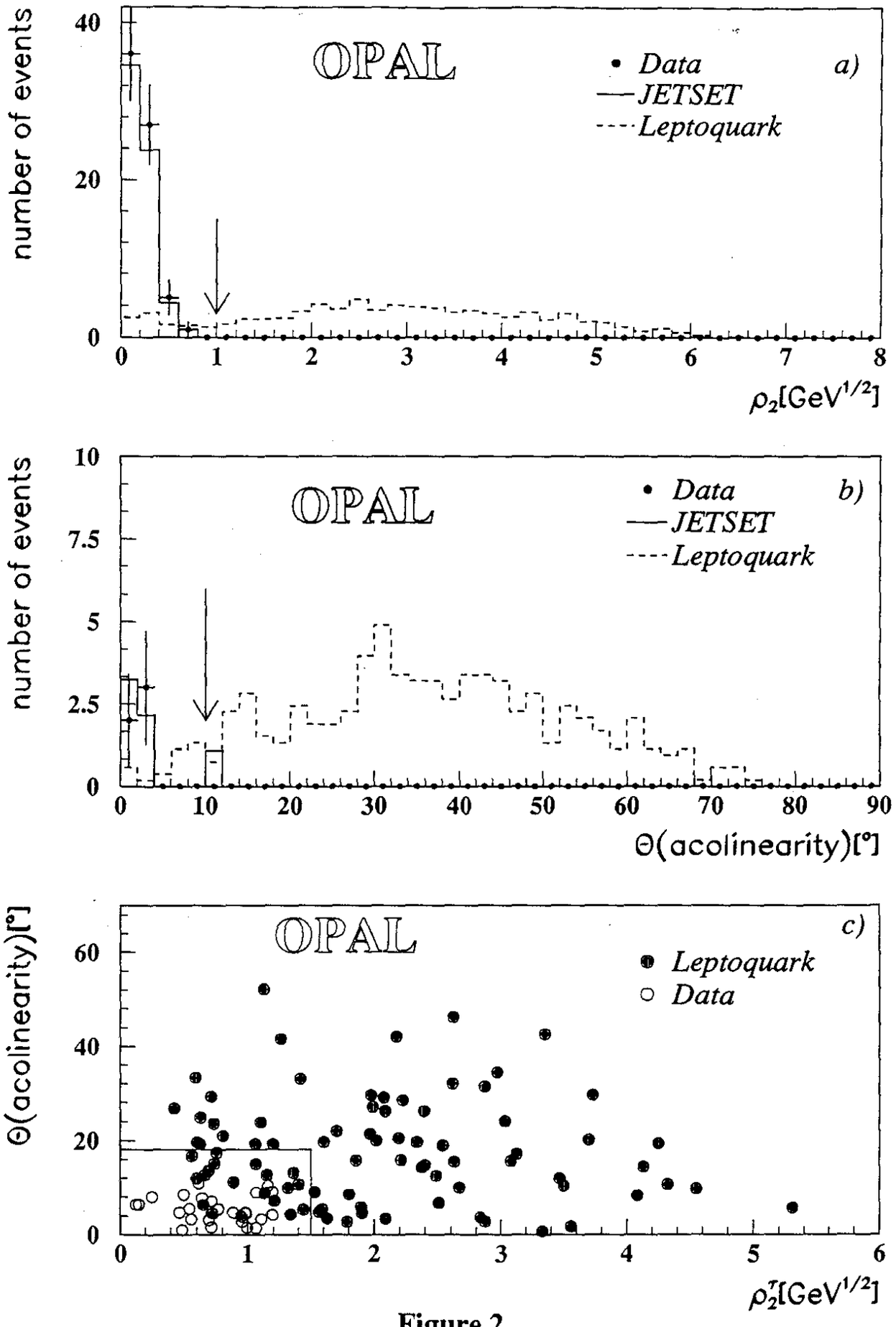
OPAL
• Data
—JETSET
----Leptoquark
a)
number of events
ρ_2[GeV$^{1/2}$]
OPAL
• Data
—JETSET
----Leptoquark
b)
number of events
Θ(acolinearity)[°]
OPAL
Leptoquark
Data
c)
Θ(acolinearity)[°]
ρ_2^τ[GeV$^{1/2}$]

Figure 2

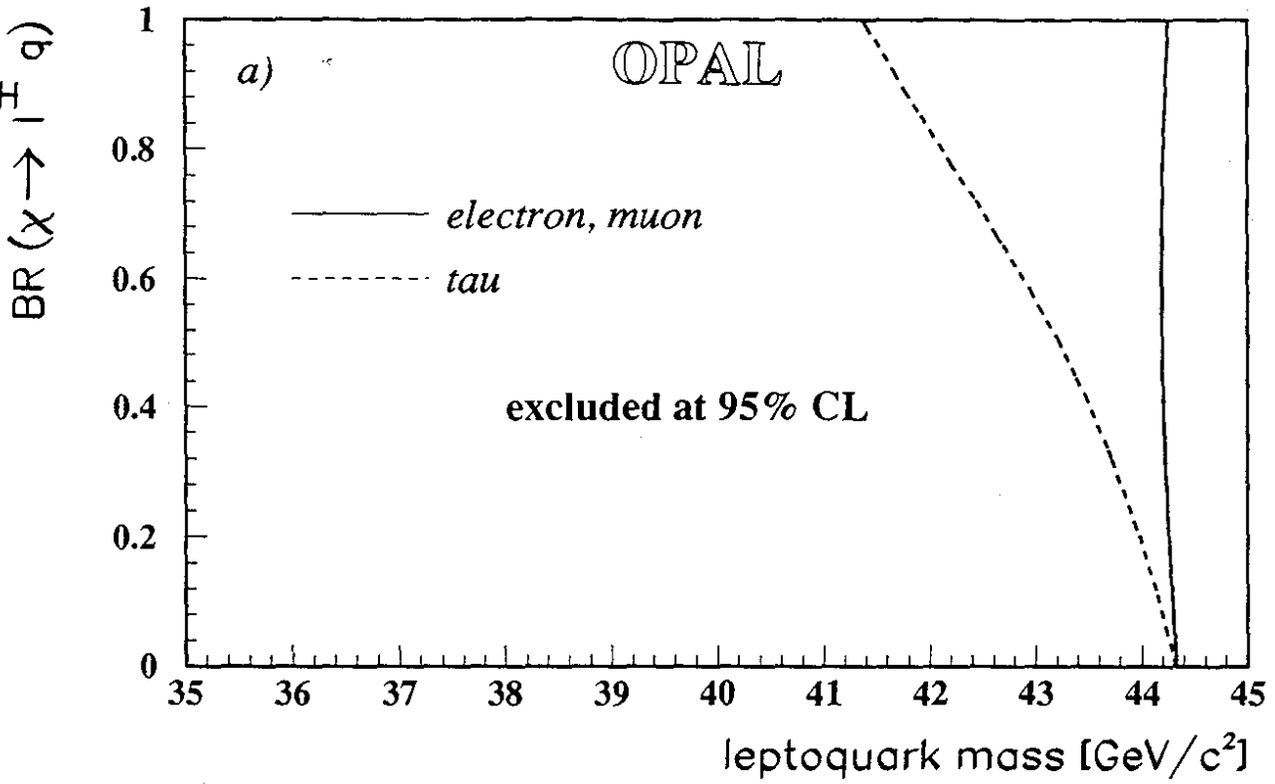
a)
OPAL
electron, muon
tau
excluded at 95% CL
BR (χ → l± q)
leptoquark mass [GeV/c²]

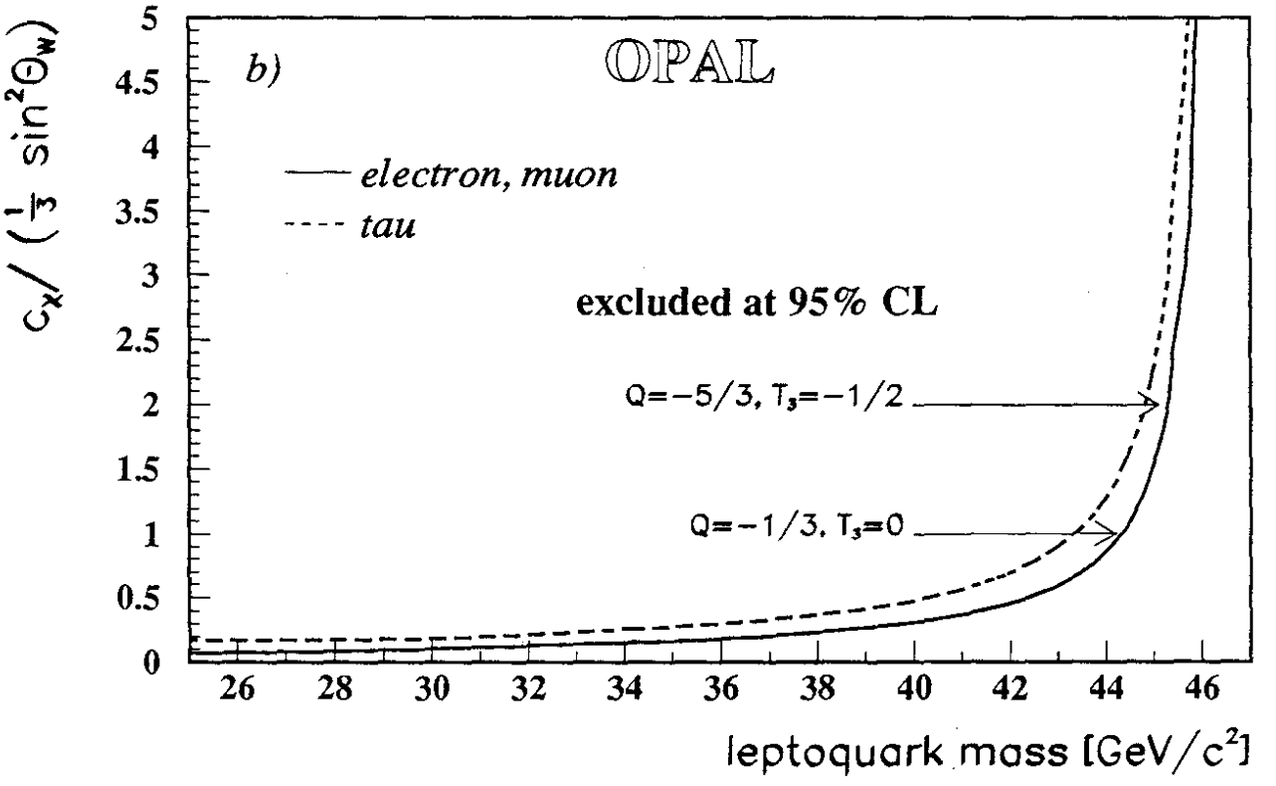
b)
OPAL
electron, muon
tau
excluded at 95% CL
Q=−5/3, T₃=−1/2
Q=−1/3, T₃=0
cχ / (⅓ sin²θW)
leptoquark mass [GeV/c²]

Figure 3